

## Magnetic effects induced by self-ion irradiation of Fe films

K. Papamihail,<sup>1,2</sup> K. Mergia,<sup>1,\*</sup> F. Ott,<sup>3</sup> Yves Serruys,<sup>4</sup> Th. Speliotis,<sup>1</sup> G. Apostolopoulos,<sup>1</sup> and S. Messoloras<sup>1</sup>

<sup>1</sup>*Fusion Technology Group, National Center for Scientific Research “Demokritos”, 15310 Athens, Greece*

<sup>2</sup>*Solid State Physics Department, Faculty of Physics, National and Kapodistrian University of Athens, 15784 Zografou, Greece*

<sup>3</sup>*Laboratoire Léon Brillouin CEA/CNRS, CEA Saclay, 91191 Gif-sur-Yvette Cedex, France*

<sup>4</sup>*Laboratoire JANNUS DEN/DMN/SRMP, CEA Saclay, 91191 Gif-sur-Yvette Cedex, France*

(Received 7 October 2015; revised manuscript received 10 February 2016; published 14 March 2016)

Iron magnetic moment enhancement is observed following the irradiation of iron films with 490 keV Fe<sup>+</sup> at room temperature. The iron magnetic moment enhancement increases to saturation with irradiation dose. The enhanced magnetic moment decays exponentially to its value before the irradiation with a time constant of 5.2 months. The iron magnetic moment enhancement is attributed to the creation of vacancy clusters having a concentration of about 20%, whereas the relaxation effects is attributed to the dissociation of these clusters.

DOI: [10.1103/PhysRevB.93.100404](https://doi.org/10.1103/PhysRevB.93.100404)

Magnetic interactions determine not only the physical but also the mechanical properties of Fe based alloys which are widely used in many applications. The magnetic interactions [1,2] are incorporated in multiscale modeling [3] aimed at predicting the properties of steels in extreme environments, e.g., fusion or fission conditions. In addition, the correlation between magnetism and mechanical strength has been proved experimentally [4]. Further, the fact that the mechanical properties of these steels deteriorate under neutron irradiation [5] leads to the inescapable conclusion that neutron irradiation must affect the long range magnetism of these alloys. The lattice damage in the case of neutron irradiation is not produced by the neutron per se, but by the primary knock-on atoms (PKAs), which in the case of steels are mainly iron atoms. As a result we can investigate the effects of neutron irradiation by employing Fe ion irradiation [6], and as a first, simplifying step it is suitable to employ pure iron as a target. It should be noted that 14 MeV neutrons have a large free mean path and PKAs with different energies are generated along their track. Ion irradiation refers to a specific PKA energy produced along the neutron path. The energy for the Fe ion irradiation was selected as 490 keV, which corresponds to the mean energy of Fe PKAs produced by fusion neutrons of 14 MeV energy. This choice was made for the following reasons: This research is part of an international effort to develop radiation resistant alloys expected to be used in future fusion power plants [7,8], combining multiscale modeling, experimental validation, and irradiation campaigns in fission reactors [9,10]. In addition, at present we have no direct knowledge of the damage produced by the 14 MeV fusion neutrons since the mean energy of fission neutrons used to study the radiation damage is about 2 MeV and, thus, the validity of extrapolating these irradiation studies to the fusion environment is questionable.

In the literature, changes in the structural and magnetic properties of iron films induced by heavy ion irradiation and/or implantation are reported [11–14]. However, in these studies no changes in the magnetization were reported. This is attributed either to the existence of implantation effects [13,14], which is not the case in the current work, or the use of

much lower fluences (two orders of magnitude lower) [11,12] than in the current work.

Ion bombardment of an Fe target by 490 keV Fe<sup>+</sup> results in both damage and implantation, and these two effects were simulated using the SRIM software [15] and a displacement energy of 40 eV (ASTM standard [16]). From these simulations it was determined that up to a depth of 60 nm the implantation of Fe<sup>+</sup> in Fe is negligible and, on the other hand, the radiation damage produced is very high. Thus, iron films having a thickness of 60 nm were fabricated on one side polished (100) single crystal MgO and (001) silicon wafer substrates using dc magnetron sputtering. A Cr cover layer having a nominal thickness of 4 nm was deposited on top of the Fe layer in order to prevent oxidization. Irradiation with a 490 keV Fe<sup>+</sup> ion beam were performed at the JANNUS facility at CEA-Saclay using an ion flux of around  $2 \times 10^{12}$  ions/(cm<sup>2</sup>s). The samples during the irradiation were placed on a liquid nitrogen cooled flange, compensating for the heating induced by the beam and, thus, keeping the samples' temperature at 25 °C. The damage is characterized in terms of the total number of times that an individual atom is initially displaced from its lattice site, i.e., “displacements per atom” (dpa), and this unit is employed throughout this paper. The dpa does not acknowledge the number of interstitials recombining with vacancies, i.e., the remaining Frenkel pairs are indicated by Norgett, Robinson and Torrens (NRT) dpa [17]. The dpa values are determined by employing the integrated number of recoils, given by SRIM simulations, over the Fe film depth. The samples were irradiated for different doses which correspond to a dpa range from 1.5 to 72. The corresponding atomic density increase due to the Fe ion implantation was from  $0.6 \times 10^{-3}\%$  to 0.28%.

The individual films were characterized before and after the irradiation on both the structural and magnetic properties. The structural characterization was carried out by x-ray reflectivity (XRR) and x-ray diffraction both at normal and grazing incidence angle. The x-ray scattering measurements were performed on a D8 Advance Bruker diffractometer using Cu K $\alpha$  radiation and a parallel beam stemming from a Göbel mirror. The magnetic state of the samples was determined by vibrating sample magnetometry (VSM) and polarized neutron reflectivity (PNR) measurements. Magnetic hysteresis loop measurements are used to determine the magnetic properties of the total film thickness, whereas the magnetic moment

\*Corresponding author: [kmergia@ipta.demokritos.gr](mailto:kmergia@ipta.demokritos.gr)

per atom versus depth is determined by PNR. The PNR measurements were performed on the PRISM spectrometer at the Laboratoire Léon-Brillouin, CEA-Saclay. An in-plane external magnetic field of 1.2 T was applied in order to align the magnetic domains. The incident neutron wavelength was 0.40 nm and the  $Q$  range varied from 0.05 to 2.3 nm<sup>-1</sup> ( $Q$  is the magnitude of scattering vector,  $Q = k' - k$ ). In PNR measurements we obtain two reflectivities:  $R^+$ , corresponding to the spin of incident neutrons parallel to the applied magnetic field (spin up) and  $R^-$ , that corresponding to the spin being down. The spin up and down reflectivities can be calculated from the exact solution of the Schrödinger equation for an assumed model of density and magnetic moment profile versus depth. The parameters of the model are derived by a least squares fit to the experimental data using SimulReflec software [18]. During the research relaxation effects were present, so XRD, magnetization, and PNR measurements carried out at different periods from the time of the irradiation are reported.

From XRR measurements the density profile of the film versus depth is determined. From these measurements no density profile change arising from the irradiation was found. The x-ray diffraction measurements at grazing incidence angle (GIXRD) show a bcc crystalline structure of the as-fabricated Fe films which remains even after the irradiation of 72 dpa. The integrated intensity of the (110) XRD Bragg peak decreases as the dose increases, to about 25% at the maximum dose of 72 dpa. The decrease of the integrated intensity with dose indicates a loss of crystallinity. The out of plane lattice constant as measured by GIXRD coincides, within an error bar, with the lattice constant measured with normal XRD. From peak profile analysis the grain size was calculated [19].

Both the lattice constant and the grain size as a function of dose (Fig. 1) increase monotonically until they reach saturation at about 15 dpa. The grain size varies between 20 nm, for the nonirradiated sample, up to 30 nm for the 72 dpa irradiation. The lattice constant for the unirradiated film is 0.2% below the Fe bulk value and after 10 dpa irradiation it reaches the Fe bulk value. This indicates the existence of 0.2% compressive strains in the as-fabricated Fe films, and as the irradiation

dose increases the strains are relieved. A similar strain value, for the same Ar pressure (3 mTorr), is found for magnetron sputtered Fe films in the work of Javed *et al.* [20]. Moreover, the coincidence of the lattice constant as determined from XRD and GIXRD measurements indicates that the stress is isotropic. From Fig. 1 an initial stage is observed where the lattice constant and the grain size increase abruptly, in addition to a second stage where both properties gradually approach the saturation. The variation of the lattice constant and the grain size versus dose,  $d$ , in dpa, show the same dose dependence, which can be described by a simple empirical equation,

$$\frac{p(d) - p_0}{p_{\max} - p_0} = 1 - \exp\left(-\frac{d}{d_h}\right), \quad (1)$$

where  $p$  is the property in question (i.e., either lattice constant or grain size) and  $p_0$  and  $p_{\max}$  are the property values for zero and maximum dose, respectively. For the lattice constant,  $p_{\max} = 2.8669(3) \text{ \AA}$  and  $p_0 = 2.861(1) \text{ \AA}$ , and for the grain size,  $p_{\max} = 30.4(5) \text{ nm}$  and  $p_0 = 20.0(5) \text{ nm}$ . The constant  $d_h$  is obtained from the least squares fit of Eq. (1) to the data of both the lattice constant and grain size and has the value  $d_h = 2.5(4) \text{ dpa}$ . The fitted curve according to Eq. (1) is presented in Fig. 1 as a solid line. It should be stressed that despite the good fitting of Eq. (1) to the data, the mathematical formulation is only indicative of the dose dependence of the lattice constant and grain size. Ion irradiation has been observed to induce grain growth in thin polycrystalline metal film and it has been theoretically investigated in a number of studies (see Refs. [21–25] and references therein). Grain growth by ion irradiation may be caused by increased atomic mobility, indirectly through mobile radiation induced crystal defects and directly through atomic collisions. The role of each mechanism in ion irradiation enhanced grain growth is still unclear.

The structural changes of the Fe films caused by the 490 keV Fe<sup>+</sup> irradiation can be summarized as follows: The bcc crystal structure remains overall even at the dose of 72 dpa. However, there is a loss of crystallinity. The density of the films within the 10% accuracy of the XRR measurements is unaffected by the irradiation. However, there is a lattice expansion and grain growth. Both the lattice constant and grain size increase follow the same growth equation [Eq. (1)] versus irradiation dose. This correlation of grain size and lattice constant increase versus defect production (in dpa) is an important finding which demonstrates that any models of radiation damage should aim at explaining not only the alteration of physical properties arising from the irradiation, but also the correlation of the induced changes as depicted in Fig. 1.

In Fig. 2 the magnetization hysteresis loop of a 60 nm Fe film is shown in its as-fabricated state and after 72 dpa, 490 keV Fe<sup>+</sup> irradiation. We observe a considerable increase in the magnetization up to about 32%. Fe films irradiated with lower doses show a smaller increase of the magnetization and this will be discussed in the following paragraphs. In order to have an accurate determination of the magnetic moment per atom and, more importantly, to examine whether there is a magnetic profile, we carried out PNR measurements.

The Fe magnetic moment determined from the PNR measurements for the unirradiated specimen was found to be equal to  $2.1\mu_B/\text{atom}$ . This value is of about 5% lower than that expected for the bulk Fe at room temperature calculated

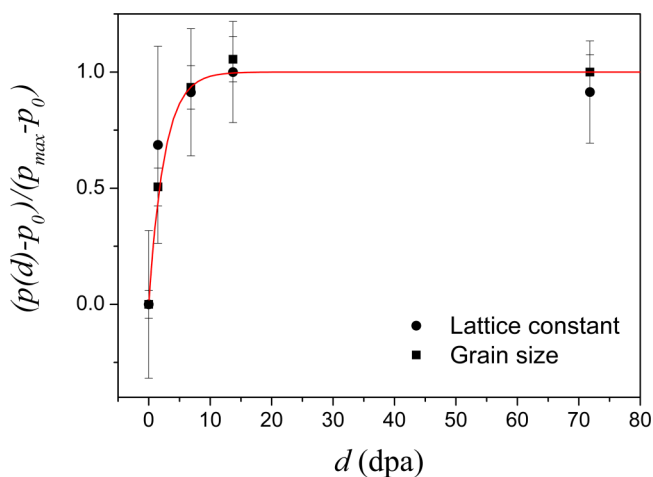


FIG. 1. Normalized lattice constant and grain size as a function of dose. The solid line is a least squares fit of Eq. (1) to the data (see text for details).

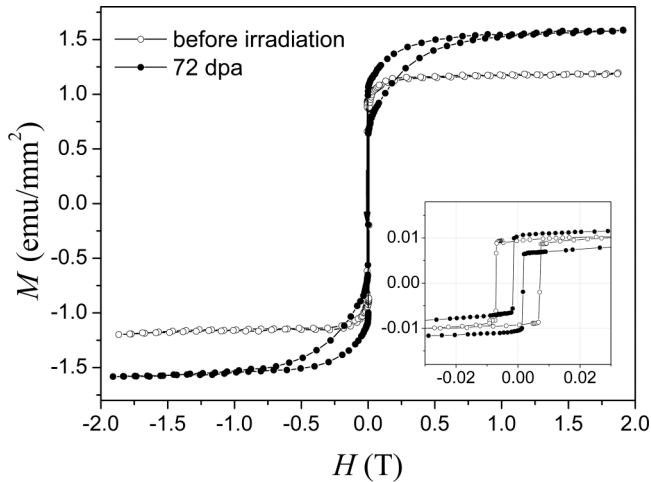


FIG. 2. Magnetization hysteresis curves: (a) open circles before irradiation and (b) solid circles after 72 dpa irradiation with 490 keV  $\text{Fe}^+$ . The inset is a zoom in of the hysteresis loop around zero field.

from its magnetization versus temperature curve [26]. From the magnetic hysteresis loop (Fig. 2) we observe that the magnetic field of 1.2 T used for the PNR measurements results in a magnetization around 5% lower than the saturation value. Taking this into consideration, it can be concluded that the PNR determination of the Fe magnetic moment in the 60 nm iron films agrees extremely well with the value of bulk iron at room temperature.

The spin up and spin down reflectivities for the sample irradiated at 72 dpa are shown in Fig. 3. The reflectivities have been multiplied by  $Q^4$  in order to remove the asymptotic  $1/Q^4$  dependence. From a least squares fit to both cross sections (solid line in Fig. 3) the magnetic moment of the Fe film irradiated at 72 dpa was determined to be  $2.5\mu_B/\text{atom}$ . In order to show the accuracy of the magnetic moment determination, two simulations with lower and higher magnetic moment values are shown in Fig. 3. We estimate that the accuracy of the

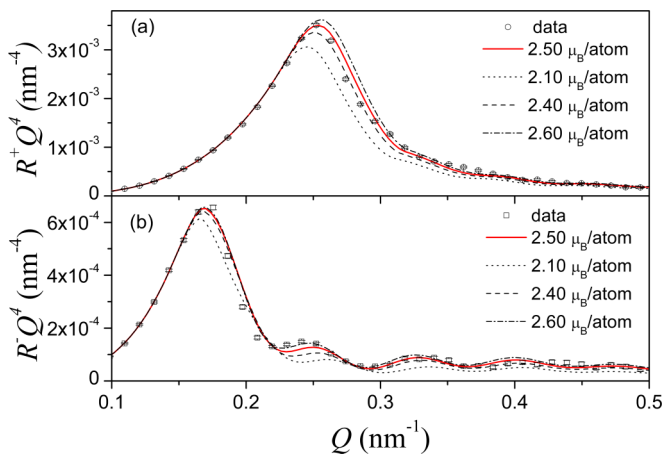


FIG. 3. (a)  $R^+Q^4$  and (b)  $R^-Q^4$  data versus the scattering vector. The solid line is a least squares fit to the data corresponding to a magnetic moment for Fe of  $2.5\mu_B/\text{atom}$ . The dotted, dashed, and dashed-dotted lines correspond to models with Fe magnetic moments of  $2.1\mu_B/\text{atom}$ ,  $2.4\mu_B/\text{atom}$ , and  $2.6\mu_B/\text{atom}$ , respectively.

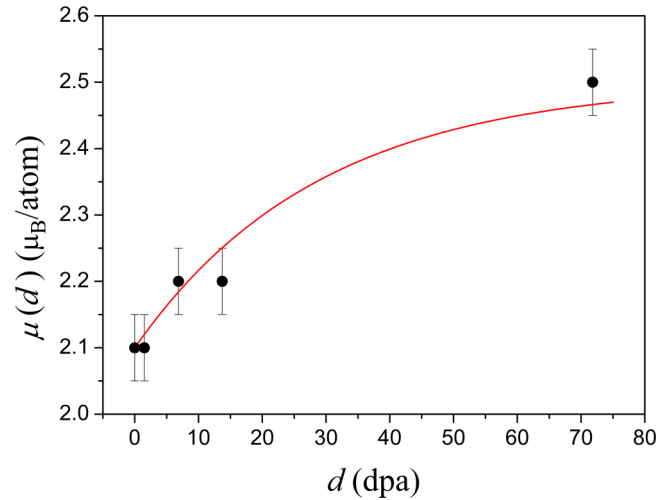


FIG. 4. Atomic magnetic moment as a function of dpa. The solid line is a least squares fit of Eq. (1) (see text for details).

magnetic moments per atom derived by PNR measurements is around 2.5%. In Fig. 3 we also show the calculated PNR curve for a Fe magnetic moment of  $2.1\mu_B/\text{atom}$ , the value we found for the unirradiated sample (see above). Comparison of this with the experimental data leaves no doubt regarding the increase of the magnetic moment after 72 dpa  $\text{Fe}^+$  irradiation. In this stage some aspects of the PNR techniques must be brought to the reader's attention. PNR is very sensitive in determining magnetic or density variations versus depth with a resolution of about 0.1 nm, but it averages over the  $x$ - $y$  plane. Within this resolution it should be mentioned that no magnetic profile versus depth was found. Thus, the determined magnetic moment is an average over the film volume. This means that either all the atoms have the determined magnetic moment value or there are regions of higher and lower magnetic moments per atom dispersed randomly over the whole volume of the sample having as a mean the determined value.

The variation of the atomic magnetic moment,  $\mu$ , determined by PNR versus ion dose in dpa,  $d$ , is depicted in Fig. 4. The magnetic moment versus dose data,  $\mu(d)$ , were fitted using Eq. (1), i.e.,  $p(d) = \mu(d)$ , and  $\mu_0 = 2.1\mu_B/\text{atom}$  is the value determined for the unirradiated samples and  $\mu_{\text{max}} = 2.5\mu_B/\text{atom}$  that determined for the sample irradiated at 72 dpa. The least squares determined value for  $d_h$  was  $31 \pm 6$  dpa. Notwithstanding that the magnetic moment increase versus dose follows the same increase law as that of the grain size and lattice constant, its increase is much slower. It should be emphasized that the fitting of Eq. (1) to the data illustrates only an overall pictorial description and in no way implies a mathematical exactness. For a more comprehensive description, denser experimental data points are required.

Measurements of the magnetization hysteresis loop and the PNR curves at different times after the irradiation showed that the magnetic moment exhibits relaxation effects. The magnetic moment of the Fe film irradiated at 72 dpa versus time measured from the end of the irradiation is shown in Fig. 5, along with both PNR and VSM. The magnetization from the VSM measurements has been converted to  $\mu_B/\text{atom}$  using the thickness and mass density as determined by the

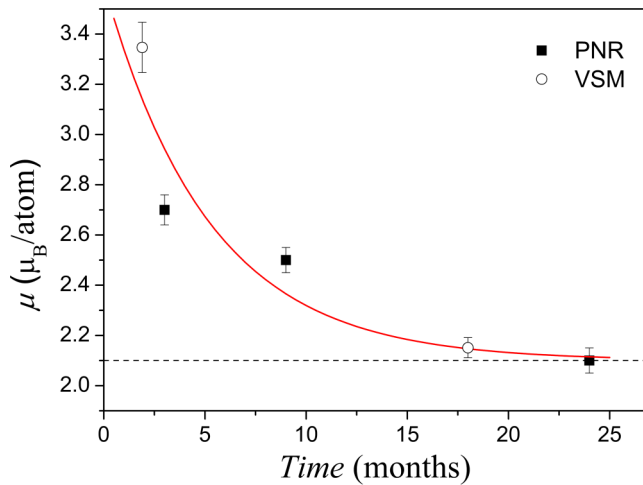


FIG. 5. Atomic magnetic moment of the Fe film irradiated at 72 dpa as a function of the time elapsed from the  $\text{Fe}^+$  irradiation. The solid line is a least squares fit to the data of Eq. (2).

XRR measurements. The solid line in Fig. 5 is a least squares fit of the data to the equation

$$\mu(t) = \mu_{\text{ref}} + \mu_0 \exp\left(-\frac{t}{t_h}\right), \quad (2)$$

where  $\mu_{\text{ref}}$  is the magnetic moment of the sample before the irradiation, i.e.,  $2.1\mu_B/\text{atom}$ . From the least squares fit the parameters  $\mu_0$  and  $t_h$  were  $1.5 \pm 0.4\mu_B/\text{atom}$  and  $5.2 \pm 2.0$  months, respectively. Considering the time dependence of the magnetic moment (Fig. 5), it should be mentioned that the variation of the magnetic moment versus dose in Fig. 4 corresponds to a time of 9 months elapsed from the end of the sample irradiation. Figure 4 refers to the determination of the magnetic moment of all the irradiated samples by PNR measurements which were carried out 9 months after their irradiation [27]. Only the sample irradiated at 72 dpa was measured by PNR after 3 and 9 months [28], and the values are shown in Fig. 5.

To conclude the spectacular effects of  $\text{Fe}^+$  irradiation on the magnetic properties of the Fe films, we refer to the decrease in the coercive field as for example this is seen in the inset of Fig. 2, where the initial value of 70 Oe has changed to 13 Oe after 72 dpa. The coercive field versus dose shows an exponential decrease. This is not surprising as it was found that the coercive field  $H_c$  and the grain size  $w$  are well correlated, i.e.,  $H_c(w) \propto b/w$ , and by least squares it was found that  $b = (3.18 \pm 0.13)$  Oe  $\mu\text{m}$ .

The drastic increase of the Fe magnetic moment revealed by magnetization and PNR measurements is quite unexpected. A reasonable starting point for explaining the magnetic moment increase would be to attribute it to an atomic volume increase. The increase of the magnetic moment with increasing atomic

volumes has been shown by *ab initio* calculations [29,30]. Using the empirical formula [2]  $\mu = \mu_c(1 - \sqrt{v_c/v})^\gamma$  ( $v$  is the atomic volume and  $v_c$  a critical atomic volume corresponding to the onset of ferromagnetism), the observed magnetic moment of  $2.5\mu_B/\text{atom}$  after 72 dpa corresponds to an atomic volume of  $15.5 \text{ \AA}^3$ . A lattice expansion after irradiation has been observed in the current study; however, the atomic volume that corresponds to 72 dpa is merely  $11.8 \text{ \AA}^3$ , close to that of bulk iron. Intuitively we may imagine that a region rich of vacancies which increases the averaged atomic volume would have the same result. A concentration of vacancies around 20% would give a mean atomic volume of  $15.5 \text{ \AA}^3$  and thus an average magnetic moment per Fe atom of  $2.5\mu_B$ . It has been found by atomistic computer simulations in  $\alpha$ -Fe that second- and third-nearest-neighbor vacancy dimers are stable energetically and larger vacancy clusters can be formed by combinations of the triangular trimers and the square tetramers on the  $\{100\}$  plane [31]. Also, from kinetic Monte Carlo simulations it was found that vacancy clusters are mobile, having increasing with their size energy for migration and dissociation [32]. Therefore, it is plausible to assume that the observed increase of the magnetic moment arises from the presence of vacancy clusters. These vacancy clusters would have the effect of reducing the local electronic density  $\rho$ . Correlating the magnetic moment with the electronic density described by a simple model [1], we find that reduction of the relative electronic density  $\rho/\rho_c$  ( $\rho_c$  is a density corresponding to the onset of ferromagnetism) from 0.83 to 0.74 corresponds to an increase of the magnetic moment from  $2.1\mu_B/\text{atom}$  to  $2.5\mu_B/\text{atom}$ . As a result of attributing the increase of the Fe magnetic moment after the irradiation to the presence of vacancy clusters, the relaxation effects can be explained straightforwardly as being due to the lifetime of these clusters.

We have offered a plausible explanation of the unexpected, drastic increase of the Fe magnetic moment after irradiation with 490 keV  $\text{Fe}^+$ . However, many questions remain to be answered by further experiments and calculations. A central question is what types of defect complexes, e.g., vacancy clusters, remain after an irradiation with 490 keV  $\text{Fe}^+$  and what their lifetimes are. In this work the necessary information for detailed future calculations is provided, since, in addition to the relaxation time and magnetic moment, the lattice constant and grain size are given.

This work was funded by the European Commission under the Contract of Association between EURATOM and the Hellenic Republic Association, and was carried out within the framework of the European Fusion Development Agreement. The views and opinions expressed herein do not necessarily reflect those of the European Commission. This research has been supported by the European Commission under the Seventh Framework Programme (FP7) through Key Action: Strengthening the European Research Area, Research Infrastructures, Contract No. NMI3-II/FP7 No 283883.

[1] S. L. Dudarev and P. M. Derlet, *J. Comput. Aided Mater. Des.* **14**, 129 (2007).

[2] P. M. Derlet and S. L. Dudarev, *Prog. Mater. Sci.* **52**, 299 (2007).

- [3] M. Victoria, S. Dudarev, J. L. Boutard, E. Diegele, R. Lässer, A. Almazouzi, M. J. Caturla, C. C. Fu, J. Källne, L. Malerba, K. Nordlund, M. Perlado, M. Rieth, M. Samaras, R. Schaeublin, B. N. Singh, and F. Willaime, *Fusion Eng. Des.* **82**, 2413 (2007).
- [4] K. Mergia and N. Boukos, *J. Nucl. Mater.* **373**, 1 (2008).
- [5] S. J. Zinkle and N. M. Ghoniem, *J. Nucl. Mater.* **417**, 2 (2011).
- [6] G. S. Was and R. S. Averback, *Radiation Damage Using Ion Beams in Comprehensive Nuclear Materials* (Elsevier, New York, 2012), Vol. 1.07, p. 195.
- [7] R. Lässer, N. Baluc, J.-L. Boutard, E. Diegele, S. Dudarev, M. Gasparotto, A. Möslang, R. Pippan, B. Riccardi, and B. van der Schaaf, *Fusion Eng. Des.* **82**, 511 (2007).
- [8] M. Gasparotto, R. Andreani, L. V. Boccaccini, A. Cardella, G. Federici, L. Giancarli, G. Le Marois, D. Maisonnier, S. Malang, A. Möslang, Y. Poitevin, B. van der Schaaf, and M. Victoria, *Fusion Eng. Des.* **66-68**, 129 (2003).
- [9] D. Stork, P. Agostini, J. L. Boutard, D. Buckthorpe, E. Diegele, S. L. Dudarev, C. English, G. Federici, M. R. Gilbert, S. Gonzalez, A. Ibarra, Ch. Linsmeier, A. Li Puma, G. Marbach, P. F. Morris, L. W. Packer, B. Raj, M. Rieth, M. Q. Tran, D. J. Ward, and S. J. Zinkle, *J. Nucl. Mater.* **455**, 277 (2014).
- [10] S. J. Zinkle, J. P. Blanchard, R. W. Callis, C. E. Kessel, R. J. Kurtz, P. J. Lee, K. McCarthy, N. B. Morley, F. Najmabadi, R. E. Nygren, G. R. Tynan, D. G. Whyte, R. S. Willms, and B. D. Wirth, *Fusion Eng. Des.* **89**, 1579 (2014).
- [11] Y. Kamada, H. Watanabe, S. Mitani, J.-i. Echigoya, H. Kikuchi, S. Kobayashi, N. Yoshida, and K. Takanashi, *Mater. Trans.* **50**, 2134 (2009).
- [12] Y. Kamada, H. Watanabe, S. Mitani, J. Echigoya, J. N. Mohapatra, H. Kikuchi, S. Kobayashi, and K. Takanashi, *J. Phys.: Conf. Series* **266**, 012035 (2011).
- [13] G. A. Müller, E. Carpena, R. Gupta, P. Schaaf, K. Zhang, and K.P. Lieb, *Eur. Phys. J. B* **48**, 449 (2005).
- [14] K. P. Lieb, K. Zhang, G. A. Müller, R. Gupta, and P. Schaaf, *Hyperfine Interact.* **160**, 39 (2005).
- [15] J. F. Ziegler, J. P. Biersack, and U. Littmark, *The Stopping and Range of Ions in Solids* (Pergamon, New York, 1985) (SRIM-2008 code: <http://www.srim.org/>).
- [16] ASTM E693-94: Standard Practice for Characterizing Neutron Exposures in Iron and Low Alloy Steels in Terms of Displacements Per Atom (DPA), E706(ID) (ASTM International, West Conshohocken, PA, 1991).
- [17] M. I. Norgett, M. T. Robinson, and I. M. Torrens, *Nucl. Eng. Des.* **33**, 50 (1975).
- [18] <http://www-llb.cea.fr/prism/programs/simulreflec/simulreflec.html>, version 1.9.
- [19] M. Birkholz, *Thin Film Analysis by X-ray Scattering* (Wiley-VCH, Weinheim, 2006).
- [20] A. Javed, N. A. Morley, and M. R. J. Gibbs, *Appl. Surf. Sci.* **257**, 5586 (2011).
- [21] D. Kaoumi, A. T. Motta, and R. C. Birtcher, *J. ASTM Int.* **4**, 1 (2007).
- [22] D. E. Alexander and G. S. Was, *Phys. Rev. B* **47**, 2983 (1993).
- [23] D. Kaoumi, A. T. Motta, and R. C. Birtcher, *J. Appl. Phys.* **104**, 073525 (2008).
- [24] J. C. Liu and J. W. Mayer, *Nucl. Instrum. Methods B* **20**, 538 (1987).
- [25] N. Karpe, J. Böttiger., N. G. Chechenin, and J. P. Krog, *Mater. Sci. Eng. A* **179-180**, 582 (1994).
- [26] Soshin Chikazumi, *Physics of Magnetism* (Wiley, New York, 1964).
- [27] K. Mergia, K. Papamihail, F. Ott, Th. Speliotis, G. Apostolopoulos, Y. Serruys, and S. Messoloras, Polarised Neutron Reflectivity Reveals Enhanced Magnetic Moment of Fe<sup>+</sup> Irradiated Iron Films, Laboratoire Léon Brillouin, CEA/CNRS, 2013 Annual Report, [http://www-llb.cea.fr/fr-en/Annual\\_Repport\\_LL\\_B\\_2013.pdf](http://www-llb.cea.fr/fr-en/Annual_Repport_LL_B_2013.pdf).
- [28] The PNR measurement after 3 months was a trial experiment and the second set of extended measurements after an application procedure to Laboratoire Léon Brillouin, CEA/CNRS, and approval of experimental time by a panel of experts.
- [29] H. C. Herper, E. Hoffmann, and P. Entel, *Phys. Rev. B* **60**, 3839 (1999).
- [30] M. Černý, J. Pokluda, M. Šob, M. Friák, and P. Šandera, *Phys. Rev. B* **67**, 035116 (2003).
- [31] F. Ye, C. Yin, K. Tong, C. Zhang, and W. B. Liu, *Mater. Res. Innov.* **18**, S4-1003 (2014).
- [32] F. G. Djurabekova, L. Malerba, C. Domain, and C.S. Becquart, *Nucl. Instrum. Methods B* **255**, 47 (2007).